SEVIER

Journal of Power Sources 61 (1996) 227–237

JOURNAL OF POWER SOURCES

atalytic activity and stability of heat-treated iron phthalocyanines for the electroreduction of oxygen in polymer electrolyte fuel cells

G. Lalande [a], G. Faubert [a], R. Côté [a], D. Guay [a], J.P. Dodelet [a], L.T. Weng [b], P. Bertrand [b]

[a] *INRS–Energie et Matériaux, CP 1020, Varennes, Qué., J3X 1S2 Canada*

[b] *PCPM, Université Catholique de Louvain, 1, Place Croix du Sud, 1348 Louvain-la-Neuve, Belgique*

stract

ron phthalocyanine (FePc) and tetracarboxylic iron phthalocyanine (FePcTc) have been adsorbed on carbon black (C). The resulting
c/C and FePcTc/C have been heat-treated in Ar at various temperatures ranging from 100 to 1100 °C to obtain catalysts for the
ctroreduction of oxygen. The electrochemical properties of these materials have been measured by rotating disk electrode and in polymer
ctrolyte fuel cells. These properties have been correlated with the bulk and surface characterizations of the catalysts. The most active
alyst is unpyrolyzed FePcTc/C but it is also the least stable one. The only catalysts which are active and stable are those obtained at high
olysis temperatures ($\geq$900 °C). At those temperatures there is no Fe–N bond anymore, and Fe is mainly observed as a metal surrounded
a graphitic envelope. After 10 h in a fuel cell at 50 °C, 0.5 V versus reversible hydrogen electrode (RHE), FePcTc/C and FePc/C pyrolyzed
000 °C yielded currents 37 and 40% that of a commercial Pt catalyst containing the same metal loading (2 wt.%), respectively.

words: Phthalocyanines; Electroreduction; Oxygen; Polymer electrolyte fuel cells; Iron

Introduction

Polymer electrolyte fuel cells (PEFCs) with their charac-
istic high efficiency, very low or zero emission and fuel
xibility, offer the best prospects for potentially replacing
internal combustion engine in all areas of ground trans-
rtation [1–4]. However, remaining technical challenges
ve to be overcome before PEFCs become an attractive
onomical alternative to the conventional sources of elec-
:al energy for vehicles. Among these challenges, the reduc-
n of component costs (membrane, catalysts, etc.) is
portant.

Pt and its alloys are electrocatalysts for hydrogen oxidation
d oxygen reduction in today's low temperature fuel cells.
though Pt is recoverable after the useful life of the fuel cell,
present production rate of Pt will be sufficient for only
% of the automobiles manufactured today in the USA (on
basis of 20 g of Pt per vehicle) if they were all to be
uipped with PEFCs [5]. There have been several attempts
replace Pt as the electrocatalyst for the reduction of oxygen
PEFCs. One promising avenue is the use of transition metal
icrocycles either unpyrolyzed or pyrolyzed. Several
iews have been published on the topic [6–10].

We undertook a study concerning the electrocatalytic prop-
ies for oxygen reduction of chelate precursors adsorbed on
:bon black and heat-treated at various temperatures. These chelates were Co phthalocyanine (CoPc) [11–16], tetracarboxylic Co phthalocyanine (CoPcTc) [17] and Co tetraphenylporphyrin (CoTPP) [18]. The study was recently extended to Fe tetraphenylporphyrin (FeTPP) [18]. The goals of these studies were (i) to identify the nature of the catalytic site for oxygen reduction and (ii) to determine the behavior of these catalysts in fuel cells (activity and stability).

It was found that the nature of the catalytic site depends on the heat-treatment temperature: it is the metal–N_4 moiety (or its fragments) in the low and median temperature range but, in the high temperature range ($\geq$900 °C), where metal–N bonds are not detected anymore, metallic clusters surrounded by several layers of graphite are observed. They are believed to be the catalytic centers for the catalysts prepared at high pyrolysis temperatures. The high temperature catalysts also display much better stability in fuel cell life tests.

Recently, we showed that iron-based catalysts prepared from FeTPP loaded on carbon black (FeTPP/C) and pyrolyzed at 900 °C displayed about 65% of the activity of a commercial platinum catalyst containing the same amount of metal (2 wt.%). Since iron-based catalysts seem to be more interesting in terms of activity and stability than Co based ones, we decided to extend our studies to other iron-based macrocycle precursors like Fe phthalocyanine (FePc) and

PII S0378-7753(96)02356-7

tetracarboxylic Fe phthalocyanine (FePcTc). The latter chelate was added to determine the effect of oxygen on the catalytic properties.

2. Experimental

2.1. Preparation of FePc/C and FePcTc/C

Iron phthalocyanine (FePc) was prepared by the method of Muto and Horiguchi [19]. The reaction was carried out under Ar. Briefly, $FeCl_2$ (2.54 g), phthalonitrile (10.2 g) and tributylphosphine (5 ml) were dissolved in 100 ml of anhydrous ethylene glycol. The solution was refluxed for 30 min and cooled down to room temperature. The crystalline solid was filtered and rinsed with methanol. It was then suspended in a mixture of 150 ml of methanol and 8 ml of formic acid (96%) to be refluxed for 30 min before being hot filtered, rinsed and dried in air at 70 °C. FePc was purified by two vacuum sublimations at 520 °C and 10^{-6} torr. The synthesis and purification of FePcTc will be reported elsewhere.

FePc and FePcTc were adsorbed onto carbon black (XC-72R from Cabot) according to the following procedure: in order to obtain catalysts containing 2 wt.% Fe, 0.12 g FePc or 0.19 g FePcTc were dispersed with 0.5 g of XC-72R in 40 ml of anhydrous pyridine. The dispersion was stirred at reflux for 8 h under Ar. The slurry was then poured into 1 l of deionized water to precipitate the organic precursor onto the carbon black. For FePcTc, the precipitation was completed by lowering the pH to 2 with formic acid. The resulting material was then filtered, rinsed with de-ionized water and dried overnight at 75 °C in air.

The catalysts were then heat-treated under Ar for 2 h at temperatures ranging from 100 to 1100 °C. In order to eliminate aging problems, the samples were stored under Ar or vacuum. When the catalysts were stored in such conditions, no difference in activity was observed over a 6-month period, as was previously reported [20].

2.2. Electrochemical measurements

The catalysts were evaluated electrochemically in half- and full-cells. Measurements in half-cell were obtained by the rotating disk electrode technique (RDE). The experimental setup and procedure are described in detail elsewhere [13]. Briefly, 10 mg of finely ground catalyst, 0.400 ml of deionized H_2O and 0.400 ml of a Nafion recast solution (5 wt.% in alcohol–water solution) were ultrasonically blended for 10 min. Then, 10 μl of this suspension were pipetted onto the 0.196 cm^2 glassy carbon disk of the electrode. The suspension was dried in air at 75 °C.

RDE measurements were performed at room temperature in H_2SO_4 at pH 0.5. Cyclic voltammograms were carried out with an AFRDE-4 bipotentiostat and an AFMMSRX rotating disk speed controller from Pine Instruments. The voltammograms were recorded from 0 to 0.70 V versus saturated calomel electrode (SCE) at a scan rate of 10 mV/s. The catalytic activity was determined by taking the difference between the current measured at 0.46 V (0.70 V versus NHE) when the electrode is rotating at 1500 rpm and when it is stationary.

Measurements in full-cells were obtained with gas diffusion electrodes (GDE) in a fuel cell test station. The catalyst suspension for the cathode consisted of 17.1 mg of catalyst, 0.240 ml of de-ionized H_2O and 0.240 ml of 5 wt.% Nafion recast solution blended ultrasonically for 1 h. The resulting thick paint was applied in 4 successive layers on a 1 cm^2 uncatalyzed ELAT electrode from ETEK (Natick, MA). Each layer consisted of 60 μl of the catalyst suspension. The paint was dried in air at 60 °C between the application of each layer and in a vacuum oven at 70 °C for 1 h after the deposition of the last coating. The iron metal loading in these cathodes was about 0.15 mg/cm^2.

The anode consisted of a 1 cm^2 ELAT electrode catalyzed with 0.37 mg/cm^2 (20 wt.%) Pt from ETEK. A single cell assembly was prepared by pressing a Nafion 117 membrane between the anode and the cathode under 2500 psi at 140 °C for 40 s.

All fuel cell measurements were performed at 50 °C. H_2 and O_2 gases, both humidified in water bubblers at 75 °C were kept at a pressure of 30 and 60 psig with constant flow rates of 95 and 100 cm^3/min, respectively. Before performing any measurements, the fuel cell assembly was left under open circuit for 1 h. Next, the impedance was measured (EGG potentiostat, model 273 and EGG Lock-in analyser, model 5206). Typical values obtained varied from 0.4 to 0.5 Ω. Then a polarization curve was recorded by varying an applied potential from 0.9 to 0 V versus RHE. This was followed by the application of a steady potential of 0.5 V versus RHE for 10 h to ascertain the stability of the catalysts.

2.3. Surface analysis

X-ray photoelectron spectroscopy analysis (XPS) was performed on a VG Escalab MK II, using the Mg Kα line (1253.6 eV). The powdered samples were mounted on a conductive copper tape. No charging problems were encountered except for pure FePc and pure FePcTc. Photoelectron spectra were recorded for the C(1s), N(1s), O(1), $Fe2p_{3/2}$ and $Fe2p_{1/2}$ core levels of the Fe-containing catalysts. All spectra were referenced to the C(1s) level of the carbon black at 284.35 eV. A semiquantitative analysis of the XPS results was performed using the relation $C_x = (I_x C_x)/(I_c S_c)$ where C_x, I_x or I_c and S_x or S_c are the atomic surface concentration ratio, the areas under the elemental XPS peak, and the sensitivity factors for the element x or for carbon, respectively [21].

The surfaces of the FePc/C and FePcTc/C based catalysts were also probed by time-of-flight secondary ion mass spectrometry (ToF-SIMS). ToF-SIMS measurements were performed with a spectrometer from Charles Evans and Assocs. Ga^+ primary ions were accelerated onto the samples at 15

keV. The secondary ions were first accelerated to ± 10 keV by a bias applied between the sample and the extraction lens. Deflection of the emitted secondary ions into three electrostatic analysers controlled the spreading of the initial energies. After their passage in these analysers, the secondary ions were submitted to a post-acceleration electric field of ±5 kV to allow for increased sensitivity for heavy ions (> 200 atomic mass unit (amu)) in the multichannel detector. The analysed area was $100 \times 100\ \mu m^2$. The data acquisition time was 10 min on the 0–5000 amu range, giving a total ion dose inferior to 10^{12} ions/cm^2, which is lower than the usually accepted dose for static conditions [22]. No charge compensation was needed. All the samples were mounted onto an Al foil by a conductive double-sided scotch tape, except for pure FePc and FePcTc, which were directly pressed onto an In foil. The data acquisition software was from Charles Evans and Assoc. For this study, the mass resolution $M/\Delta M$ was ≅ 3000 at 29 amu. In this paper, the relative SIMS intensity of a peak refers to the ratio $I/\Sigma I_i$, where I is the integrated intensity of the considered peak, and ΣI_i is the sum of the integrated intensities of all the peaks in the considered spectrum.

2.4. TEM and XRD analyses

Transmission electron microscopy (TEM) was performed with a JEOL 2000 FX operating at 200 keV. The powdered catalyst was ultrasonically dispersed in isopropanol for 30 s. A drop of the solution was deposited onto a carbon-coated copper grid and left in air to dry.

X-ray diffraction (XRD) was performed on an automated Philips PW 1050/2S X-ray powder diffractometer automated with a Sietronics SIE system. The Ni filtered Kα radiation of Cu (λ = 1.54178 Å) was used. The powdered samples were pressed into the 21×15 mm^2 cavity of a Plexiglas holder. The X-ray diffraction patterns were collected in the $\theta/2\theta$ step scanning mode at a speed of 1°/min, with a step size of 0.02° (2θ). The Joint Committee on Powder Diffraction Standards (JCPDS) data base was referred to for peak identification.

3. Results

3.1. Electrochemical activity and stability of the catalysts

The RDE currents for O_2 reduction are presented in Fig. 1 as a function of heat-treatment temperature for FePc/C and FePcTc/C based catalysts. These RDE results were recorded at room temperature. Each experimental point represents an average between 2 to 3 measurements. The curve depicting the electroactivity of FePc/C as a function of heat-treatment temperature is similar to the electroactivity curves obtained for other chelate precursors like CoPc [13,15], CoTPP, FeTPP [18] and even CoPcTc [17]. For all these precursors, maximum electroactivity is obtained after their pyrolysis on carbon black at temperatures ranging between 500 to 700 °C. Similar results are also found in the literature [6–10].

The curve characterizing the evolution of the electroactivity for FePcTc/C is peculiar. It shows maximum catalytic activity for the unpyrolyzed catalyst or for the catalysts heat-treated up to 200 °C. The RDE currents drop drastically between 200 and 300 °C. Above 500 °C, the measured electroreduction currents for FePcTc/C based catalysts are nearly the same as those measured for FePc/C based catalysts. According to Fig. 1, unpyrolyzed FePcTc/C is the best electrocatalyst for O_2 reduction among all other precursors cited above and measured in the same experimental conditions.

Figs. 2 and 3 present the polarization curves recorded at 50 °C for the FePcTc/C and FePc/C based catalysts, respectively. For the sake of clarity, only selected temperatures are

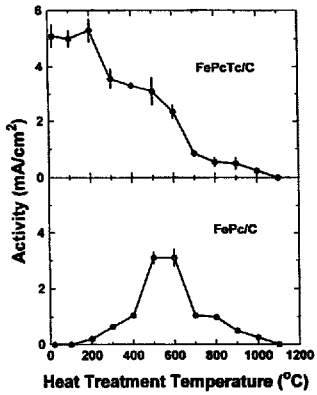

Fig. 1. Evolution of the RDE currents for O_2 reduction as a function of heat-treatment temperature for FePc/C and FePcTc/C.

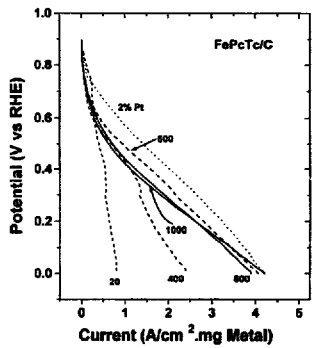

Fig. 2. Polarization curves, recorded at 50 °C, for the catalysts obtained after the heat-treatment of FePcTc/C at various temperatures: (———) stable catalysts; (— — —) unstable catalysts, and (· · ·) 2 wt.% Pt/C catalyst.

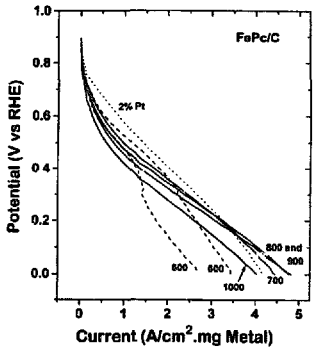

Fig. 3. Polarization curves, recorded at 50 °C, for the catalysts obtained after the heat-treatment of FePc/C at various temperatures: (———) stable catalysts; (— — —) unstable catalysts, and (· · ·) 2 wt.% Pt/C catalyst.

displayed in Fig. 2 and Fig. 3. The polarization curve of 2 wt.% Pt (dotted line), obtained using the same experimental conditions as was used for the polarization curves obtained for the 2 wt.% Fe catalysts, is added to both figures for comparison purposes.

Figs. 4 and 5 display the results of the stability tests for FePcTc/C and FePc/C based catalysts, respectively. These tests were run immediately after taking the polarization curves. They demonstrate that a stable current (or even a current rising slowly over time similar to that of 2 wt.% Pt) is obtained only after pyrolysis of the Fe precursor/C at high temperature. The polarization curves of these catalysts are represented by full lines in Figs. 2 and 3. On the other hand, the polarization curve for the catalysts incapable of sustaining stable currents in Figs. 4 and 5 are represented by broken lines in Figs. 2 and 3. A peculiar case is the one of unpyrolyzed FePcTc/C, which was found to be the most active of

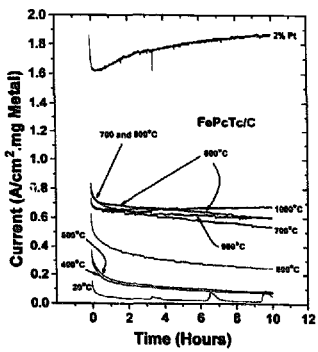

Fig. 4. Short term stability tests performed at 0.5 V on the catalysts obtained after the heat-treatment of FePcTc/C at various temperatures.

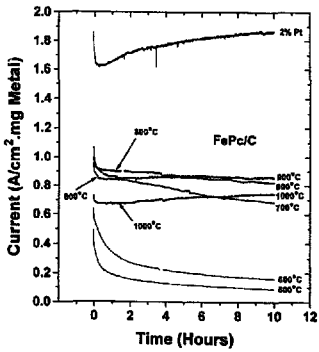

Fig. 5. Short term stability tests performed at 0.5 V on the catalysts obtained after the heat-treatment of FePc/C at various temperatures.

all FePcTc/C based catalysts (Fig. 1) during RDE (low current) testing. Its polarization curve starts, indeed, above that of 2 wt.% Pt in the low current region. However, it loses its activity rapidly as soon as larger reduction currents are drawn from the gas diffusion electrode. The stability tests show that unpyrolyzed FePcTc/C displays the lowest activity among all the catalysts measured in this work.

3.2. Chemical and physical characterization of the catalysts

A series of chemical and physical characterizations were undertaken in order to ascertain the nature of the catalytic site and to explain the electrocatalytic behavior of the heat-treated organometallic precursors adsorbed on carbon black.

3.2.1. Bulk Fe and N dosimetry

Fig. 6 shows the evolution, as a function of heat-treatment temperature, of bulk Fe and N concentrations for FePc/C and FePcTc/C based catalysts. This evolution is similar for both types of precursors. Roughly speaking, bulk Fe concentrations remain practically constant in the entire range of temperatures, whereas bulk N concentrations decrease as the temperature increases. The latter reaches the detection threshold of 0.5 wt.% at 900 °C. The drop in bulk N concentrations is especially drastic above 600 °C. It corresponds to the massive departure from the surface of the catalyst of molecular fragments containing nitrogen. Indeed, it will be shown later on by ToF-SIMS that FePc, for instance, pyrolyzes completely between 500 and 600 °C.

3.2.2. Fe and N surface concentrations

Fig. 7 shows the evolution, as a function of heat-treatment temperature, of surface Fe and N concentrations for FePc/C and FePcTc/C based catalysts. Both Fe and N surface concentrations are expressed relative to carbon, which is the main component of the catalysts. From Fig. 7, it can be observed:

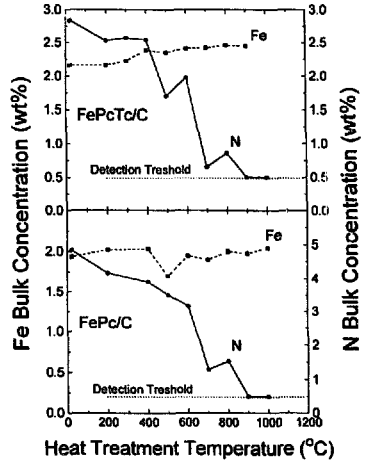

Fig. 6. Evolution of bulk Fe and N concentrations for FePc/C and FePcTc/C with the heat-treatment temperature.

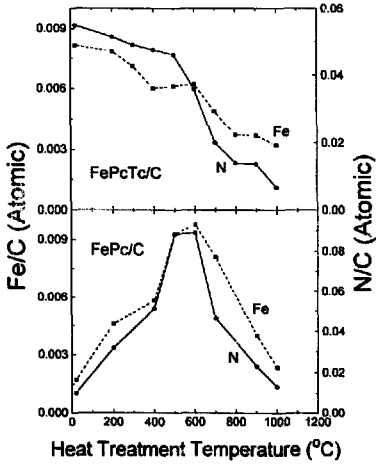

Fig. 7. Evolution of the Fe and N surface concentrations (relative to C) for FePc/C and FePcTc/C with the heat-treatment temperature.

(i) that Fe and N concentrations follow the same behavior for both precursors, and (ii) that the evolution of Fe and N surface concentrations with the temperature is similar to the evolution of the electrocatalytic activity of the same precursors with the temperature; for FePc/C, there are maxima in Figs. 1 and 7 located between 500 and 600 °C, while maximum electroactivity and Fe or N surface concentrations are observed for unpyrolyzed FePcTc/C.

3.2.3. Oxygen bulk and surface concentrations

Fig. 8 presents the evolution of bulk and surface concentrations for oxygen in FePcTc/C based catalysts with the heat-treatment temperature. The surface analyses were performed by XPS (following the O/C atomic ratio) and by ToF-SIMS (following the O^- normalized peak intensity). The three parts of Fig. 8 carry the same information: (i) the O bulk or surface concentrations decrease with the heat-treatment temperature; (ii) most of the O concentration drop occurs between 20 and 400 °C where a polymerization reaction occurs. In that temperature range, oxygen is lost by the departure of H_2O, CO or CO_2. The polymerization is complete at about 400 °C.

Thermogravimetric analysis (TGA) and differential scanning calorimetry (DSC) measurements performed on CoPcTc [17] indicated that the dehydration reaction, which initiates the polymerization of the molecule, starts at 200 °C. The second reaction begins at about 305 °C, and is associated with the loss of CO_2 and CO. That reaction was near completion at the end of the temperature ramp (400 °C). These results, although obtained for CoPcTc, are in agreement with the evolution of the oxygen bulk and surface concentrations displayed in Fig. 8 for FePcTc. It may be concluded that FePcTc and CoPcTc follow the same polymerization steps. Above 400 °C, FePcTc seems to behave exactly like FePc as

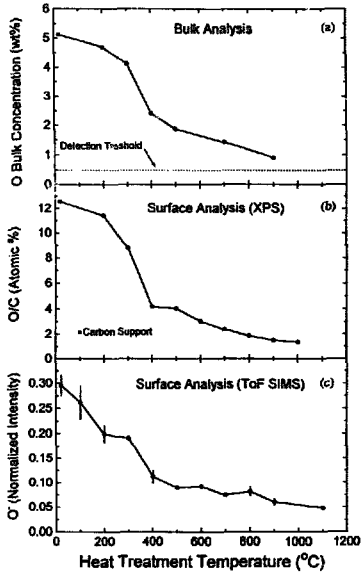

Fig. 8. Evolution of the bulk and surface concentrations of oxygen for FePcTc/C with the heat-treatment temperature.

indicated by the activity curves of Fig. 1 and the N or Fe surface concentrations of Fig. 7.

Oxygen detected above 400 °C belongs mainly to the oxygenated groups of the carbon black. Their concentration decreases slowly with increasing temperature. For the sake of comparison, the O/C concentration detected by XPS for the sole carbon black support and heat-treated at 100 °C is measured at 2 at.%.

3.2.4. ToF-SIMS results

ToF-SIMS results are important to establish the nature of the catalytic site for O_2 reduction. By ToF-SIMS, it is possible to follow the evolution of the molecular ions or molecular fragments at the surface of the catalysts with the heat-treatment temperature. It is therefore possible to deduce from these results which chemical bonds of the precursor still survive after pyrolysis at a given temperature.

It is possible to group all the ions detected by ToF-SIMS according to three types. They are: (i) molecular ions (type 3); (ii) molecular fragments containing Fe and at least one N (type 2). The presence of these ions indicates that the FeN_4 moiety of the chelate is probably still present at the surface of the carbon black; (iii) Fe^+ ion or small molecular fragments that do not contain Fe bound to N (type 1).

Fig. 9 shows the evolution of the normalized intensity of some representative with the heat-treatment temperature for FePc/C based catalysts. Tables 1 and 2 give some examples of positive and negative ions of the three types for FePc/C and FePcTc/C based catalysts as well as the pyrolysis temperature at which the ion signal is lost. From these tables it follows: (i) that molecular ions (type 3) persist until 500 °C for FePc/C based catalysts but they disappear at 600 °C. For FePcTc/C, molecular ions are not detected anymore above 200 °C. This result is in agreement with the TGA and DSC studies of CoPcTc [17]. Since it is expected that FePcTc behaves like CoPcTc, a dehydration reaction is expected to occur between 200 and 300 °C; (ii) that type 2 ions completely disappear from the surface of the substrate of FePc/C or FePcTc/C based catalysts for pyrolysis at 900 or 800 °C, respectively. It means that the FeN_4 chelate completely disappears at these temperatures from the surface of the catalyst. The latter comprises only inorganic Fe (metal, oxide,

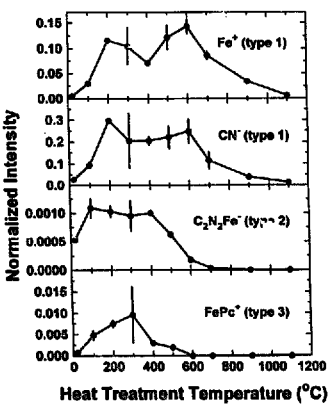

Fig. 9. Evolution of ToF-SIMS normalized intensities as a function of the heat-treatment temperature, for some typical ions detected in the spectra of FePc/C.

Table 1
Negative and positive ions and their profile type for heat-treated FePc/C

Negative ions	Atomic mass unit (amu)	Positive ions	Signal loss temperature (°C)	Profile type
CN	26.00		>1100	1
C_3N	50.00		>1100	1
C_2N_2Fe	107.94		900	2
C_7H_3Fe	115.03		900	2
C_2N_3Fe	121.94		700	2
$C_4H_2N_2Fe$	133.96		700	2
$C_{10}H_4N_3$	166.04		700	2
	55.93	Fe	>1100	1
	56.94	HFe	>1100	1
	69.95	CH_2Fe	>1100	1
	70.96	CH_3Fe	>1100	1
	71.93	FeO	>1100	1
	72.94	FeOH	>1100	1
	157.94	C_5N_3Fe	600	3
	183.97	$C_8H_4N_2Fe$	600	3
	209.99	$C_{10}H_8N_2Fe$	600	3
	568.08	FePc	600	3

Table 2
Negative and positive ions and their profile type for heat-treated FePcTc/C

Negative ions	Atomic mass unit (amu)	Positive ions	Signal loss temperature (°C)	Profile type
CN	26.00		>1100	1
C_3N	50.00		>1100	1
C_2N_2O	66.01		900	2
C_3N	74.00		>1100	1
C_2N_2Fe	107.94		800	2
C_7H_3Fe	115.03		700	2
C_2N_3Fe	121.94		700	2
C_2HN_3Fe	122.95		700	2
$C_8H_3N_2$	127.03		700	2
C_4N_2Fe	131.94		700	2
$C_4H_2N_2Fe$	133.96		700	2
C_3N_4Fe	147.95		700	2
$C_{10}H_4N_3$	166.04		700	2
	55.93	Fe	>1100	1
	56.94	HFe	>1100	1
	69.95	CH_2Fe	>1100	1
	71.93	FeO	>1100	1
	72.94	FeOH	>1100	1
	81.95	C_2H_2Fe	900	1
	96.96	C_2H_3NFe	900	1
	110.98	C_3H_3NFe	900	1
	744.04	FePcTc	300	3

carbide) giving rise to type I ions. At these temperatures, N bound to C still exists on the surface of the catalyst.

An important point to mention for the ToF-SIMS results is that all the ions from the FePc/C (or FePcTc/C) catalysts are found either in the spectrum of FePc (or FePcTc) alone or in the spectrum of the carbon black alone. This implies that the molecular fragments do not have a strong interaction with the carbon substrate.

3.2.5. $Fe2p_{3/2}$ XPS narrow scan spectra

Fig. 10 presents the $Fe2p_{3/2}$ XPS narrow scan spectra of unpyrolyzed FePcTc/C and of FePcTc/C heat-treated at various temperatures. The $Fe2p_{3/2}$ narrow scan spectrum of unpyrolyzed FePcTc/C is characterized by a broad peak with a contribution at about 708.5 eV (the energy range of Fe^{II} [23]) and another contribution at about 710.0 eV (the energy range of Fe^{III} [23]). By increasing the heat-treatment temperature of FePcTc/C up to 500 °C, the Fe^{III} contribution at 710.0 eV becomes dominant. Fe^{II} is oxidized to Fe^{III} probably by oxidizing species belonging to the carbon surface. At still higher temperatures, a peak at about 706.7 eV becomes the main feature of the spectrum. The latter feature is in the energy region characterizing either metallic Fe [23–25] or its carbides [25,26].

The $Fe2p_{3/2}$ XPS narrow scan spectra of FePc/C based catalysts are not shown because the spectra for the unpyrolyzed FePc/C and that for the heat-treated catalysts are similar to those shown in Fig. 10. For FePc/C, however, the feature at 706.7 eV never becomes a dominant peak and remains shoulder-like even at the highest pyrolysis temperature.

The presence of a large fraction of Fe^{III} in the unpyrolyzed spectrum of FePcTc/C or FePc/C might be surprising but this was previously observed by Mössbauer spectroscopy for FePc [27]. One explanation could be that the proposed first step in the FePc-mediated electroreduction of O_2 is the formation of a Fe(II)Pc–O_2 adduct with partial metal to O_2 charge transfer [28,29]. Evidence supporting this view has been provided by the matrix isolation of an O_2–FePc adduct which was unambiguously characterized spectroscopically at 15 K [30]. There is, however, no spectroscopic evidence for the presence of molecular oxygen bound to the FePc lattice at room temperature [29], and the Fe^{III} signal in the XPS spectra is attributable rather to the μ-oxo-derivatives of FePc or FePcTc.

Fig. 11 presents the N(1s) XPS narrow scan spectra obtained for FePcTc/C heat-treated at various temperatures. An equivalent set of spectra was obtained for FePc/C. There is nearly no change in the N(1s) spectra from 20 to 600 °C. The spectra consist of a single peak at 398.6 eV (397.4 eV for FePc/C), indicating that the eight nitrogen atoms in the macrocycle are equivalent. Niwa et al. [31], who studied the N(1s) spectra of various azaporphyrins and phthalocyanines, report a N(1s) peak for FePc at 399.2 eV instead of at 397.4 eV in the present work (reference value of C(1s) at 284.8 eV). The lower photoelectron energy may be due to the adsorption of the macrocycle on the carbon black.

A second peak appears at 400.6 eV (399.7 eV for FePc/C) after pyrolyzing FePcTc/C at 700 °C or above. This second peak becomes as important as the peak at 397.4 eV at 900 °C. The presence of a second peak at 700 °C confirms that the macrocycle and especially the N_4Me moiety of the chelate begin to decompose at that temperature. There are now two kinds of nitrogen atoms on the carbon support possessing a difference in their N(1s) photoelectron energy of about 2 eV.

At least two hypotheses may be presented in order to assign these nitrogen peaks. The first hypothesis concerns pyrrole-type nitrogen and aza-type nitrogen. These two types of nitrogen have been observed for H_2Pc (at 398.9 and 400.4 eV) and for H_2TPP (at 398.2 and 400.4 eV) [31]. In our case,

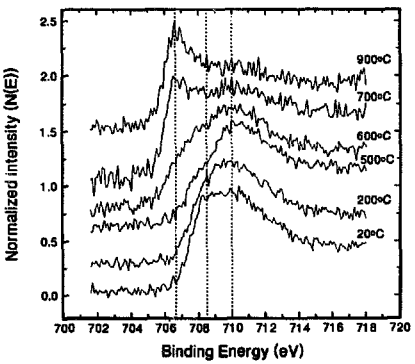

Fig. 10. Evolution of the XPS narrow scan spectra of $Fe2p_{3/2}$ as a function of the heat-treatment temperature for FePcTc/C.

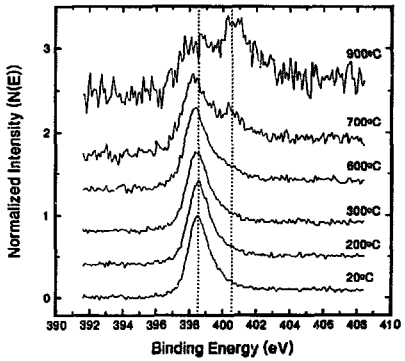

Fig. 11. Evolution of the XPS narrow scan spectra of N(1s) as a function of the heat-treatment temperature for FePcTc/C.

the appearance of the two peaks in about the same positions in the XPS spectra may be explained by the appearance of similar nitrogens (of the pyrrole- and the aza-types) in the fragments generated at high temperature. The second hypothesis concerning the assignment of a nitrogen peak at high energy would be the appearance of a protonated nitrogen in the decomposition products of the organic precursors pyrolyzed at high temperature. Protonation experiments of FePc with formic acid yield indeed, two nitrogen peaks, one at 398.6 eV and another one at 400.1 eV [32].

3.2.6. XRD diffractograms

The XRD diffractogram of FePcTc/C after pyrolysis at 1100 °C is presented in Fig. 12. The same figure also shows the diffractogram of XC-72R at the same temperature as well as the expected positions and relative intensities of four materials (α-Fe, γ-Fe, $Fe_{0.98}O$ and FeC). These materials were selected from the JCPDS database because the positions and the relative intensities of their diffraction lines constitute plausible matches to the observed experimental diffraction pattern. The closeness of the fit between the observed diffraction pattern and the patterns reported in the database was the criterion used to include or rule out the presence of a material in FePcTc/C pyrolyzed at 1100 °C. From Fig. 12, one may deduce that the main peak of the diffractogram can be assigned to α-Fe. A small contribution from γ-Fe to the XRD is also noticed as well as a still smaller contribution from $Fe_{0.98}O$. The carbide content of the catalyst is difficult to evaluate because most of the FeC diffraction peaks overlap other α-Fe or γ-Fe peaks. Although the main diffraction peaks of Fe_3C would fit the two major diffraction lines seen in Fig. 12 (around $2\theta = 45°$), it was not considered because its diffraction spectrum also displays two large satellite lines at about 37.5 and 48°, where only very small features are seen on the experimental diffractogram.

Carbides are, however, expected from the presence of γ-Fe in the catalyst. Indeed, carbon is quite soluble (up to 8 C at.%) in γ-Fe, which is the stable Fe phase at 1100 °C, compared with its solubility (nearly 0) in α-Fe, which is the stable Fe phase at room temperature [33]. Carbon atoms occupy the octahedral interstices in γ-Fe [34]. The XRD of Fig. 12 shows that the major phase is α-Fe. In equilibrium conditions and upon cooling from 1100 °C, the γ-Fe phase reaches an eutectic at 3.2 at.% C and 738 °C. Lowering the temperature further generates mainly α-Fe but also some FeC in a α-Fe/FeC ratio of 0.94. The presence of γ-Fe in Fig. 12 indicates, however, that a fraction of the high temperature phase is still present at room temperature and that the system was cooled somehow out of equilibrium conditions.

The XRD diagram of FePc/C pyrolyzed at 1100 °C (not shown) is similar to the XRD diagram of FePcTc/C shown in Fig. 12. The main differences lie in the nearly complete absence of γ-Fe and the disappearance of the oxide peaks (clearly visible in Fig. 12) into the background noise of the diffractogram. The same conclusion reached about the presence of carbides in FePcTc cooled from 1100 °C also holds for FePc/C.

The mean size of the α-Fe clusters was deduced from the XRD using the Debye–Sherrer formula. It is 11 and 9 nm for FePcTc/C and FePc/C pyrolyzed at 1100 °C, respectively.

3.2.7. TEM micrographs

Fig. 13 presents a micrograph of FePcTc/C pyrolyzed at 1100 °C. At least two Fe particles are visible on the micrograph. One is smaller than 20 nm and the other one is about 80 nm in diameter. The large particle is surrounded by a layer of lighter material that is probably graphite, on the basis of what was found for cobalt phthalocyanine loaded on carbon black and pyrolyzed at high temperature [14]. For the latter materials, several superimposed graphite layers were clearly observed around the metallic Co particles. It is difficult to

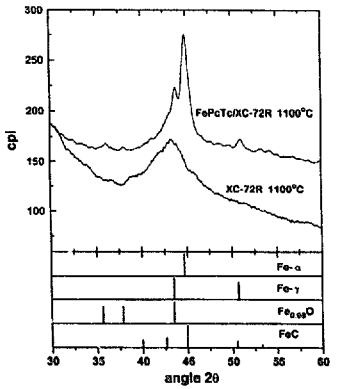

Fig. 12. XRD obtained for FePcTc/C pyrolyzed at 1100 °C along with the peak locations and relative intensities for α-Fe, δ-Fe, $Fe_{0.98}O$ and FeC.

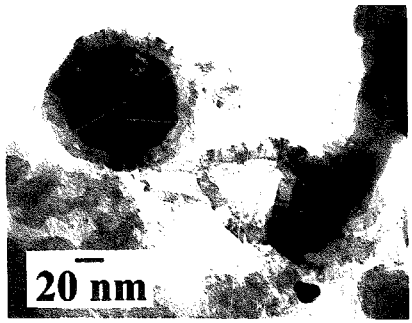

Fig. 13. TEM micrography of FePcTc/C pyrolyzed at 1100 °C.

know whether the small Fe particles in Fig. 13 are also coated by protective graphite layers. Similar results were observed for FePc/C.

4. Discussion

From the RDE (Fig. 1) and GDE (Fig. 2) results, it appears that unpyrolyzed FePcTc/C is the most active catalyst for the reduction of oxygen when the current densities are small. However, as soon as the polarization is increased (Fig. 2) to produce larger current densities in the fuel cell, unpyrolyzed FePcTc becomes the least stable of all the catalysts studied in this work. Catalysts that are active and remain stable during the 10 h life tests are obtained only after pyrolysis at high temperatures (900 °C and above). In that temperature region, there is nearly no difference between both precursors (Figs. 1–5). As a matter of fact, the behavior of both precursors becomes similar after the loss of the carboxylic oxygens (Fig. 8) and the completion of FePcTc polymerization (heat-treatment temperatures higher than 400 °C).

Looking at the RDE activity results depicted in Fig. 1, it is difficult to understand why it is interesting to study the catalysts obtained after heat-treatment at 900 °C and above. Indeed, for these catalysts, the currents measured at 0.7 V versus NHE (0.46 V versus SCE) are quite weak and even zero at 1100 °C. However, it does not mean that these materials are inactive as catalysts for oxygen reduction when larger cathodic overpotentials are applied. This fact is demonstrated in Fig. 14 which shows the voltammetric curves at 0 and 1500 rpm for unpyrolyzed FePc/C and FePc/C heat-treated at 500 and 1000 °C.

For the most active catalyst in Fig. 14 (500 °C), the 0 rpm voltammogram distinctly shows the reduction of dissolved oxygen (the peak at about 0.50 V) as well as the oxydo-reduction at 0.35 V of Fe^{II}/Fe^{III}. Macrocyclic complexes of transition metals in the oxidation state (III) undergo the following redox reaction:

$$S-Fe^{III}-OH+H_2O+e^- \rightleftharpoons S-Fe^{II}-OH_2+OH^- \quad (1)$$

The oxydo-reduction potential is pH dependent as was shown by Zagal et al. [35] for Fe tetrasulfonic phthalocyanine.

The catalysts of interest are those obtained by pyrolysis at 900 °C and above. The chemical and physical characterizations performed in this study allow us to make a few remarks about the nature of the catalytic site for these materials.

1. The active site is related to the presence of Fe and/or N on the surface of the catalysts since the evolution of Fe and N surface concentrations with pyrolysis temperature (Fig. 7) corresponds to that of the catalytic activity with pyrolysis temperature as measured by RDE (Fig. 1). The following experimental evidence will refine this first statement.
2. From ToF-SIMS experiments (Fig. 8 and Tables 1 and 2), it is possible to deduce that: (i) PcFe fragments completely disappear between 500 and 600 °C; (ii) no fragment contains Fe bound to N after pyrolysis at 900 °C of FePc/C or FePcTc/C. From these results, the active site at high pyrolysis temperatures (≥900 °C) is neither the entire precursor molecule nor a fragment of that molecule containing the FeN_4 moiety. FeN_4 is a possible catalytic site for less stable catalysts obtained at lower temperatures (<900 °C). Our XPS results at the N(1s) edge indicate, however, that FeN_4 begins to decompose at 700 °C. These results are consistent with those of Van Veen and coworkers [36–38] who proposed FeN_4 as a catalytic site for chelates pyrolyzed up to 850 °C.
3. ToF-SIMS results ascertain that the active site in the region of high pyrolysis temperatures (≥900 °C) is mainly related to the presence of Fe on the surface of the catalyst. The role of N in the catalytic activity, if it exists, is still unknown. In the region of high pyrolysis temperatures, ToF-SIMS detects ions that have their origin in inorganic Fe (metal, oxide, carbide) or of the reaction of Fe with hydrogen or hydrocarbon radicals. The presence of metallic Fe is confirmed by XPS (Fig. 10) and by XRD (Fig. 12). Furthermore, most of the metal particles seems to be surrounded with layers of graphite (Fig. 13) that

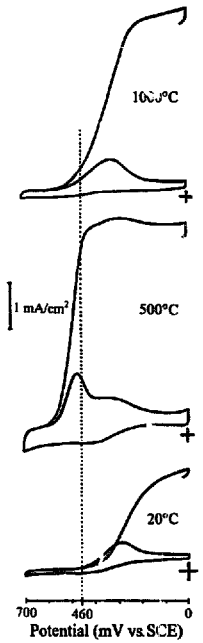

Fig. 14. Voltammetric curves at 0 and 1500 rpm for unpyrolyzed FePc/C and FePc/C heat-treated at 500 and 1000 °C.

might protect it from corrosion in acidic medium (Nafion is a perfluoropolymer sulfonic acid with a gross equivalent concentration of about 0.1 M H^+ [39]). This could explain the stability of the catalysts obtained after pyrolysis at 900 °C or above.

Since Fe remains on the catalyst irrespective of the pyrolysis temperature (Fig. 6), the decrease in catalytic activity with increasing temperature (Figs. 1–5) may be explained by the progressive increase in the size of the metallic particles. This phenomenon also explains the decrease in the Fe surface concentrations as detected by XPS (Fig. 7). When the particle sizes become larger than the escape depth of the photoelectrons, a fraction of the Fe cannot be detected anymore by XPS.

Since iron metal particles surrounded by graphite layers are the only Fe-containing compounds at these temperatures, we believe that they are the catalytic sites. A similar conclusion was already reached for catalysts obtained from other organometallic precursors like CoPc [14–16], CoPcTc [17], CoTPP and FeTPP [18]. From all these chelates, the most stable catalysts are obtained when Fe precursors are used. Among these, the catalysts obtained from FeTPP/C pyrolyzed at high temperatures are more active than those obtained from the pyrolysis of FePc/C or FePcTc/C. At 1000 °C, for instance, after 10 h at 0.5 V and 50 °C, FeTPP/C yielded 0.92 A/cm^2 mg Fe versus 0.75 and 0.68 A/cm^2 mg Fe for FePc/C and FePcTc/C, respectively.

5. Conclusions

The catalysts obtained from the heat-treatment of FePc/C and FePcTc/C are active for the electrochemical reduction of oxygen in polymer electrolyte fuel cells. The most active catalyst is unpyrolyzed FePcTc/C, but it is also the least stable one. The only catalysts which are active and stable are those obtained at high pyrolysis temperatures ($\geq$900 °C). For these temperatures, there is virtually no difference in catalytic activity between both organic precursors.

It has been demonstrated that the FeN_4 moiety of the organic precursors does not survive in the high temperature region. We therefore propose that the catalytic site is associated with the presence of inorganic Fe, mostly under metallic form and surrounded by graphite layers. However, all XPS, XRD, ToF-SIMS and TEM characterization experiments performed up to date have always been conducted on catalysts prior to their exposure to sulfuric acid solution or to Nafion. It is possible that the catalytic site may result from some in situ reaction as proposed by Yeager and co-workers [40,41]. Their model argues that upon contact with an electrolyte solution, the metal species may undergo partial or total dissolution and subsequently adsorb or coordinate to thermally formed sites on the carbon surface, in a process most likely involving nitrogen. If Fe–N_x species are formed in situ after the pyrolysis of Fe phthalocyanines at high temperatures, they should be detectable by SIMS. Experiments are in progress to verify the possible in situ formation of the catalytic site.

References

[1] P. Patil, *J. Power Sources, 49* (1994) 169.
[2] K.B. Prater, *J. Power Sources, 51* (1994) 129.
[3] K.V. Kordesch and G.R. Simader, *Chem. Rev., 95* (1995) 191.
[4] A.J. Appleby, *Int. J. Hydrogen Energy, 19* (1994) 175.
[5] S. Srinivasan, in O.J. Murphy, S. Srinivasan and B.E. Conway (eds.), *Electrochemistry in Transition*, Plenum, New York, 1992, p. 577.
[6] K. Wiesener, *Electrochim. Acta, 31* (1986) 1073.
[7] K. Wiesener, D. Ohms, V. Neumann and R. Franke, *Mater. Chem. Phys., 22* (1989) 457.
[8] M.R. Tarasevich and K.A. Radyushkina, *Mater. Chem. Phys., 22* (1989) 477.
[9] P. Vasudevan, Santosh, N. Mann and S. Tyagi, *Transition Met. Chem., 15* (1990) 81.
[10] J.H. Zagal, *Coord. Chem. Rev., 119* (1992) 89.
[11] M.C. Martin Alves, J.P. Dodelet, D. Guay, M. Ladouceur and G. Tourillon, *J. Phys. Chem., 96* (1992) 10898.
[12] M. Ladouceur, G. Lalande, D. Guay, J.P. Dodelet, L. Dignard-Bailey, M.L. Trudeau and R. Schulz, *J. Electrochem. Soc., 140* (1993) 1974.
[13] G. Tamizhmani, J.P. Dodelet, D. Guay, G. Lalande and G.A. Capuano, *J. Electrochem. Soc., 141* (1994) 41.
[14] L. Dignard-Bailey, M.L. Trudeau, A. Joly, R. Schulz, G. Lalande, D. Guay and J.P. Dodelet, *J. Mater. Res., 9* (1994) 3203.
[15] L.T. Weng, P. Bertrand, G. Lalande, D. Guay and J.P. Dodelet, *Appl. Surf. Sci., 84* (1995) 9.
[16] G. Lalande, G. Tamizhmani, R. Côté, L. Dignard-Bailey, M.L. Trudeau, R. Schulz, D. Guay and J.P. Dodelet, *J. Electrochem. Soc., 142* (1995) 1162.
[17] G. Lalande, R. Côté, G. Tamizhmani, D. Guay, J.P. Dodelet, L. Dignard-Bailey, L.T. Weng and P. Bertand, *Electrochim. Acta, 40* (1995) 2635.
[18] G. Faubert, G. Lalande, R. Côté, D. Guay, J.P. Dodelet, L.T. Weng, P. Bertrand and G. Denes, *Electrochim. Acta, 41* (1996) 1689.
[19] M. Muto and S. Horiguchi, *Jpn. Kokai, 73* (1973) 231.
[20] K. Wiesener and G. Grünig, *J. Electroanal. Chem., 180* (1984) 639.
[21] C.D. Wagner, W.M. Riggs, L.E. Davis, J.F. Moulder and G.E. Muilenberg, *Handbook of X-ray photoelectron spectroscopy*, Perkin-Elmer Corporation, Eden Prairie, Minnesota, 1978.
[22] D. Briggs and M.J. Hearn, *Vacuum, 36* (1986) 1005.
[23] L.Y. Johansson, R. Larsson, J. Blomquist, C. Cederström, S. Grapengiesser, U. Helgeson, L.C. Moberg and M. Sundbom, *Chem. Phys. Lett., 24* (1974) 508.
[24] T. Choudhury, S.O. Saied, J.L. Sullivan and A.M. Abbot, *J. Phys. D, 22* (1989) 1185.
[25] A.R. Sethuraman, J.M. Stencel, A.M. Rubel, B. Calvin and C.R. Hubbard, *J. Vac. Sci. Technol., A12* (1994) 443.
[26] J. Schwartz, P.W. Jahn, L. Wiedmann and A. Benninghoven, *J. Vac. Sci. Technol., A9* (1991) 238.
[27] A.J. Appleby, J. Fleisch and M. Savy, *J. Catal., 44* (1976) 281.
[28] F. Beck, *J. Appl. Electrochem., 7* (1977) 239.
[29] A.A. Tanaka, C. Fierro, D. Scherson and E.B. Yeager, *J. Phys. Chem., 91* (1987) 3799.
[30] T. Watanabe, T. Arna and K. Nakamoto, *J. Phys. Chem., 88* (1984) 440.
[31] Y. Niwa, H. Kobayashi and T. Tsuchiya, *Inorg. Chem., 13* (1974) 2891.
[32] T. Kawai, M. Soma, Y. Matsumoto, T. Onishi and K. Tamaru, *Chem. Phys. Lett. 37* (1976) 878.
[33] T. Lyman (ed.), *Metals Handbook, Vol. 8, Metallography, Structures and Phase Diagrams*, American Society for Metals, Metal Park, OH, USA, 8th edn., 1973.

[34] N.J. Petch, *J. Iron Steel Inst., 145* (1942) 111.
[35] J. Zagal, P. Bindra and E. Yeager, *J. Electrochem. Soc., 127* (1980) 1506.
[36] J.A.R. van Veen, J.F. van Baar and K.J. Kroese, *J. Chem. Soc. Faraday Trans. 1, 77* (1981) 2827.
[37] B. van Wingerden, J.A.R. van Veen and C.T.J. Mensch, *J. Chem. Soc. Faraday Trans. 1, 84* (1988) 65.
[38] J.A.R. van Veen, H.A. Colijn and J.F. van Baar, *Electrochim. Acta, 33* (1988) 801.
[39] A.J. Appleby, *J. Electroanal. Chem., 357* (1993) 117.
[40] D. Scherson, A.A. Tanaka, S.L. Gupta, D. Tryk, C. Fierro, R. Holze, E.B. Yeager and R.P. Latimer, *Electrochim. Acta, 31* (1986) 1247.
[41] S. Gupta, D. Tryk, I. Bae, W. Aldred and E. Yeager, *J. Appl. Electrochem., 19* (1989) 19.